Materials Letters 63 (2009) 1165–1168

Contents lists available at ScienceDirect

Materials Letters

journal homepage: www.elsevier.com/locate/matlet

Fabrication and characterization of eutectic bismuth–tin (Bi–Sn) nanowires

Shih-Hsun Chen [a], Chien-Chon Chen [b], Z.P. Luo [c,*], Chuen-Guang Chao [a]

[a] Department of Materials Science and Engineering, National Chiao Tung University, Hsinchu, Taiwan 30050, Republic of China
[b] Department of Energy and Resources, National United University, 1, Lienda, Miaoli, Taiwan 36003, Republic of China
[c] Microscopy and Imaging Center, Texas A&M University, College Station, TX 77843-2257, USA

ARTICLE INFO

Article history:
Received 22 January 2009
Accepted 12 February 2009
Available online 21 February 2009

Keywords:
Bi-Sn eutectic alloy
Electron microscopy
Microstructure
Nanowires

ABSTRACT

Eutectic Bi-43Sn (in weight percent) nanowires with diameters of 20 nm, 70 nm and 220 nm respectively, were fabricated by a hydraulic pressure injection process using anodic aluminum oxide (AAO) as templates. Novel eutectic microstructure was found within the fabricated nanowires, which are composed of alternating Bi and Sn segments along their wire axes. Within the segments, the electron diffraction analysis revealed single crystalline structures of Bi and Sn elements respectively. Parameters that control the nanowire fabrication process were discussed. It was found out that as the wire diameter reduced, longer Bi and Sn segments formed.

1. Introduction

In electronic industry, lead–tin solders have been widely used due to their favorable physical and mechanical properties, and well-developed production process [1,2]. However, concerns on the harmful Pb to the environment and human health [3] challenged the electronic industry to seek for lead-free solutions. Great efforts have been made to various tin-containing binary and ternary alloys without Pb [4,5]. Among them, a eutectic Bi-43Sn (in weight percent) alloy was recognized for its net eutectic texture, lower melting temperature (~138 °C), superior wettability, and almost void-free bonding [6–8].

Towards the miniaturization of consumer electrics and optical products, nano-scaled solders for tiny bonding with enhanced desired properties are highly demanded. It is generally accepted that reduced size and dimensionality are the critical factors in defining the material properties, which are often unforeseen in the bulk materials. Especially, one-dimensional electric materials have attracted great interest and have been extensively investigated for their unique size effects, typically fabricated using chemical reduction, chemical vapor deposition, heating in chunks, mechanical alloying, and gas pressure injection [9–14]. Recently, a new methodology by vacuum injecting process was developed, which was an easy and reproducible way to prepare metal nanowires with high efficiency [15,16]. As compared with the gas pressure injection method [9], this technique applies hydraulic pressure instead of gas compressor, and thus no surfactant is impregnated into the AAO templates along with the metal melt.

So far, limited efforts were made in nanowires with multiple components, particularly, the eutectic system. In this study, we fabricate nanowires using the eutectic Bi-43Sn solder material, and for the first time characterize the novel metallurgical microstructure of nanowires.

2. Experimental procedures

The anodic aluminum oxide (AAO) templates were fabricated by an anodization process as follows. A commercial purity aluminum plate (Al, 99.7%) was initially anodized to AAO templates using 10 vol.% sulfuric acid (H_2SO_4) at 20 V, 3 vol.% oxalic acid ($H_2C_2O_4$) at 40 V, and 1 vol.% phosphoric acid (H_3PO_4) at 160 V, to obtain pores with average diameters of 20 nm, 70 nm and 220 nm respectively. The pore depth was about 10 μm. More experimental details about the anodization process can be found in a previous research [17]. After this process, the remaining extra Al substrate serves as a support base for the brittle porous AAO template through the injection process.

The starting material for the nanowires, the eutectic Bi–Sn bulk alloy, was produced by using a vacuum smelting process. Raw materials of Bi and Sn, in the ratio of 57 wt.% Bi and 43 wt.% Sn, were sealed into a glass tube and then pumped down to high vacuum ($\sim 10^{-5}$ Torr). Afterward, the materials inside the tube were heated over their melting points to ensure both of them completely melt and well mixed into each other, and then slowly cooled down to room temperature. The bulk sample was placed into the injection apparatus, and heated up above 200 °C to melt again, and then injected into the AAO pores by a hydraulic force. Through solidification to room temperature, the eutectic Bi–Sn nanowires were formed inside the AAO template. The vacuum hydraulic pressure injection apparatus was disclosed previously [15,16].

* Corresponding author. Tel.: +1 979 845 1129; fax: +1 979 847 8933.
E-mail address: luo@mic.tamu.edu (Z.P. Luo).

0167-577X/$ – see front matter © 2009 Elsevier B.V. All rights reserved.
doi:10.1016/j.matlet.2009.02.019

Characterizations of AAO and Bi–Sn nanowires were performed by scanning electron microscopy (SEM, JEOL 6500F FESEM and FEI Quanta 600 FESEM), X-ray energy dispersive spectroscopy (EDS), X-ray diffraction (XRD, Bruker D8), differential scanning calorimeter (DSC, Perkin-Elmer Pyris 1), transmission electron microscopy (TEM, JEOL 2010 at 200 kV), and scanning TEM (STEM, FEI Tecnai G^2 F20 at 200 kV).

3. Results and discussion

The prepared starting material, bulk Bi–Sn eutectic alloy, exhibits a lamellar eutectic microstructure. A back-scattered SEM image of the bulk sample is shown in Fig. 1(a), in such an imaging mode the contrast is prepositional to the atomic number *Z*. The X-ray EDS analysis by selecting different spots confirms that the bright area in Fig. 1(a) belongs to Bi (heavier), and the dark area, Sn (lighter). The XRD pattern in Fig. 1(b) reveals that this sample composes of Bi and Sn elements only, without any binary compound. In addition, the DSC spectrum, as shown in Fig. 1(c), indicates the melting point of the Bi–Sn bulk sample at 138 °C, which is consistent to the eutectic point in the Bi–Sn phase diagram. All these results indicate that this vacuum smelting process produced a stoichiometric Bi–Sn eutectic alloy.

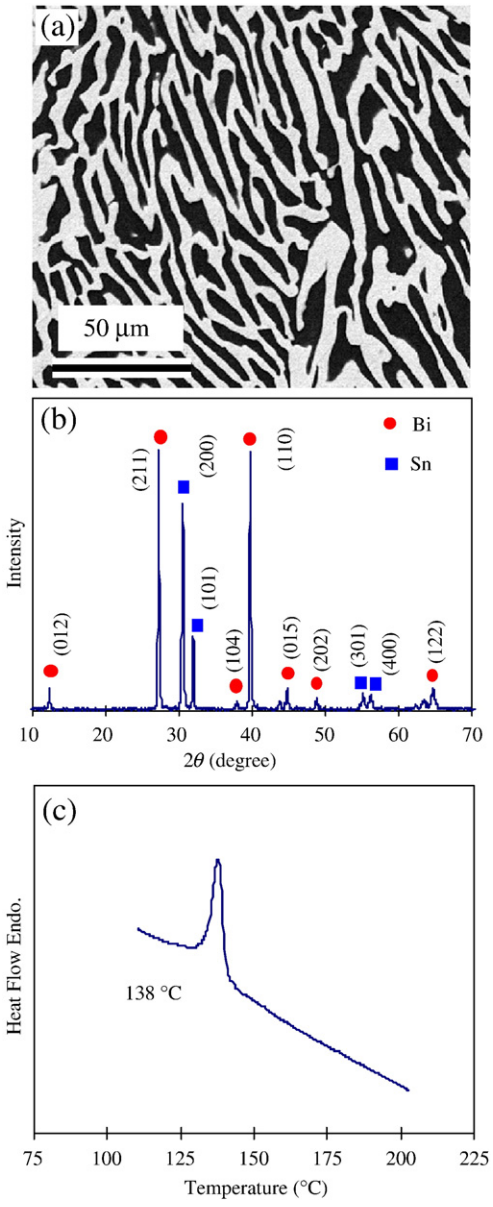

Fig. 1. Characterization of starting material. (a) Back-scattered SEM image of lamellar structure; (b) XRD spectrum showing purely Bi and Sn element peaks; (c) DSC spectrum.

Fig. 2 shows the SEM images of fabricated AAO pores (left column), nanowire bundles (middle column), and freed nanowires after dissolving the AAO template (right column), with the size of 20 nm (top row), 70 nm (middle row), and 220 nm (bottom row) respectively. The fabrication using 10 vol.% sulfuric acid as electrolyte results AAO with uniform distribution of pores, 20 nm in diameter, as shown in Fig. 2(a). The wall thickness is measured as 7 nm, and the pore density[1], ~8×10^{11} pore cm^{-2}. Using this AAO as template, Bi–Sn eutectic nanowires are obtained, as shown in the bundles in Fig. 2(b). The size of nanowires is apparently controlled by the AAO pore size. Furthermore, after dissolving the AAO using 2 wt.% sodium hydroxide (NaOH) solution for 30 min, the nanowires are freed from the AAO, as shown in Fig. 2(c). On the other hand, the AAO template, with pores of 70 nm in diameter, is fabricated by using 3 vol.% oxalic acid as electrolyte, as shown in Fig. 2(d). The pore wall thickness is found to be near 20 nm, and pore density, ~3×10^{10} pore cm^{-2}. Finally, the largest pores with 220 nm in diameter, are produced by 1 vol.% phosphoric acid, as shown in Fig. 2(g). The pore-wall thickness is about 100 nm, and the pore density, ~1×10^{9} pore cm^{-2}. Note that some residuals of the AAO template or other chemical reactants remain on the surface of some nanowires, which cause the surface roughness.

After thoroughly dissolving the AAO template, individual nanowires are deposited onto Cu grids coated with carbon support film for TEM studies. A typical nanowire, with 220 nm in diameter, is presented in Fig. 3. It exhibits alternating darker and lighter contrast. The EDS analysis reveals that the darker area belongs to Bi, and the lighter area belongs to Sn. The image contrast here is the scattering absorption contrast, so that the heavier element scatters electrons at larger angles that are filtered out by the objective aperture, and thus it shows the darker contrast. Further, the selected-area electron diffraction (SAED) patterns from the segments, as shown in Fig. 3, reveal that within the segments, the Bi and Sn are single crystals. Note that the EDS spectrum from the Sn region contains evident Bi signal, indicating a solid solution of Bi in Sn, which is consistent to the Bi–Sn phase diagram (see appendix). While the very faint Sn signal in the EDS spectrum from the Bi region may be caused by spurious X-rays from the nearby Bi areas during the EDS acquisition [18]. The signals of Al, O and P are from the surface residuals of AAO and reactants, and Cu is from the grid bar of the TEM specimen.

To ensure the observation of the eutectic microstructure, elemental mapping in the STEM model with drift correction is performed. A STEM image of the 220 nm diameter nanowires is shown in Fig. 4(a). An area is selected to map Bi and Sn elements, as shown in the magnified STEM image along with two elemental maps of Bi and Sn in Fig. 4(b). It is evident that the alternating segments within the wires are Bi and Sn elements only. When the wire diameter is reduced to 70 nm, the STEM image and elemental maps exhibit similar alternating Bi and Sn pattern, but the sections are longer than those found in the 220 nm nanowires, as shown in Fig. 5(a). The STEM image and elemental maps of the smallest 20 nm nanowires are shown in Fig. 5(b). It is seen that each nanowire, with length longer than 3 μm, only includes one or two segments within the length.

This work demonstrates that the melt injected into the AAO nanochannels, with the eutectic composition, still produces the eutectic microstructure during the solidification process, but in a confined size as segments along the wire axes. Since the fabrication methodology by mechanical injection is not compositional

[1] To measure the pore density, a large area is selected first, and then count the number of pores within this area. Dividing the pore number by the selected area defines the pore density.

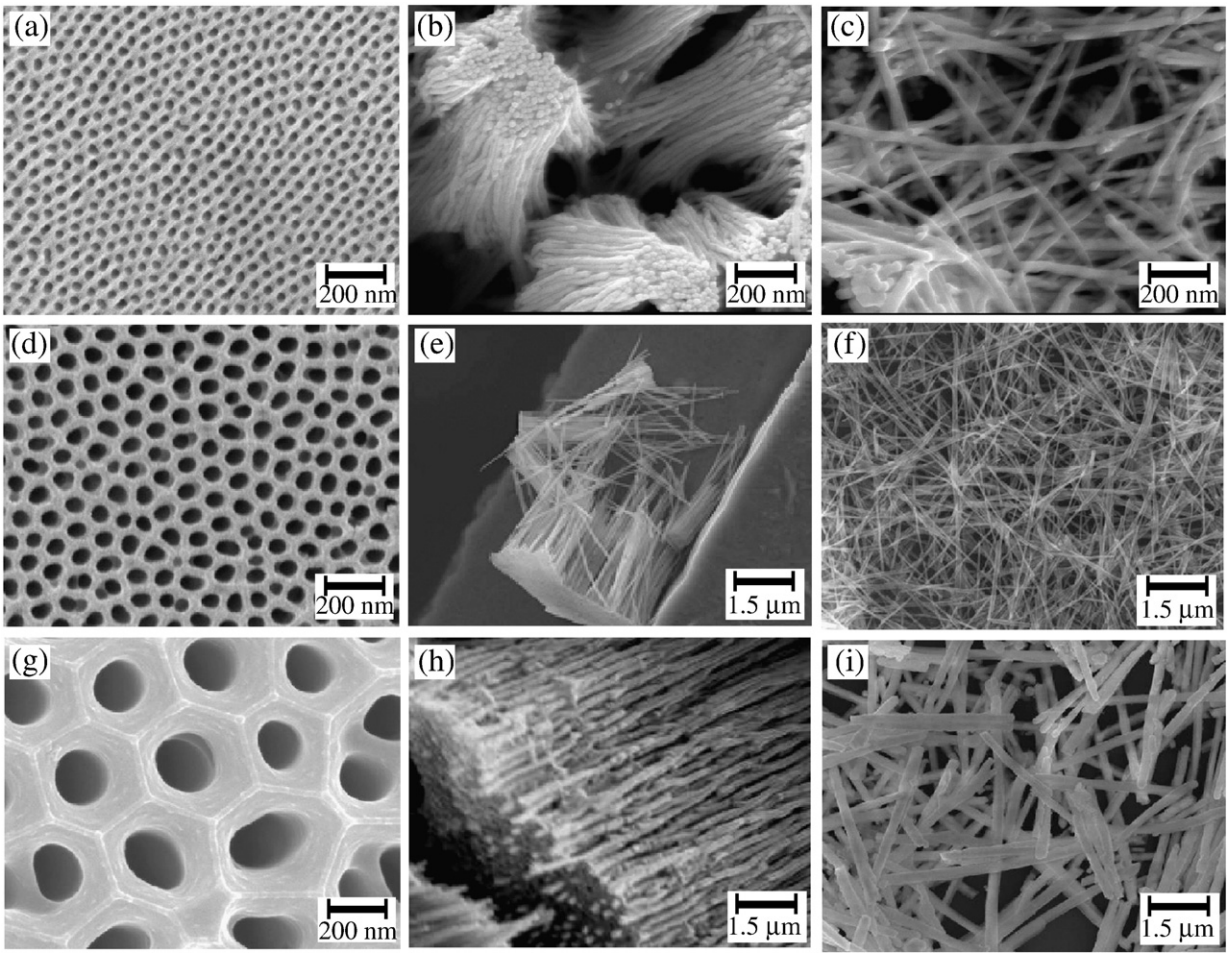

Fig. 2. SEM images of AAO pores (left column), nanowire bundles (middle column), and freed nanowires (right column), with the size of 20 nm (top row), 70 nm (middle row), and 220 nm (bottom row) respectively.

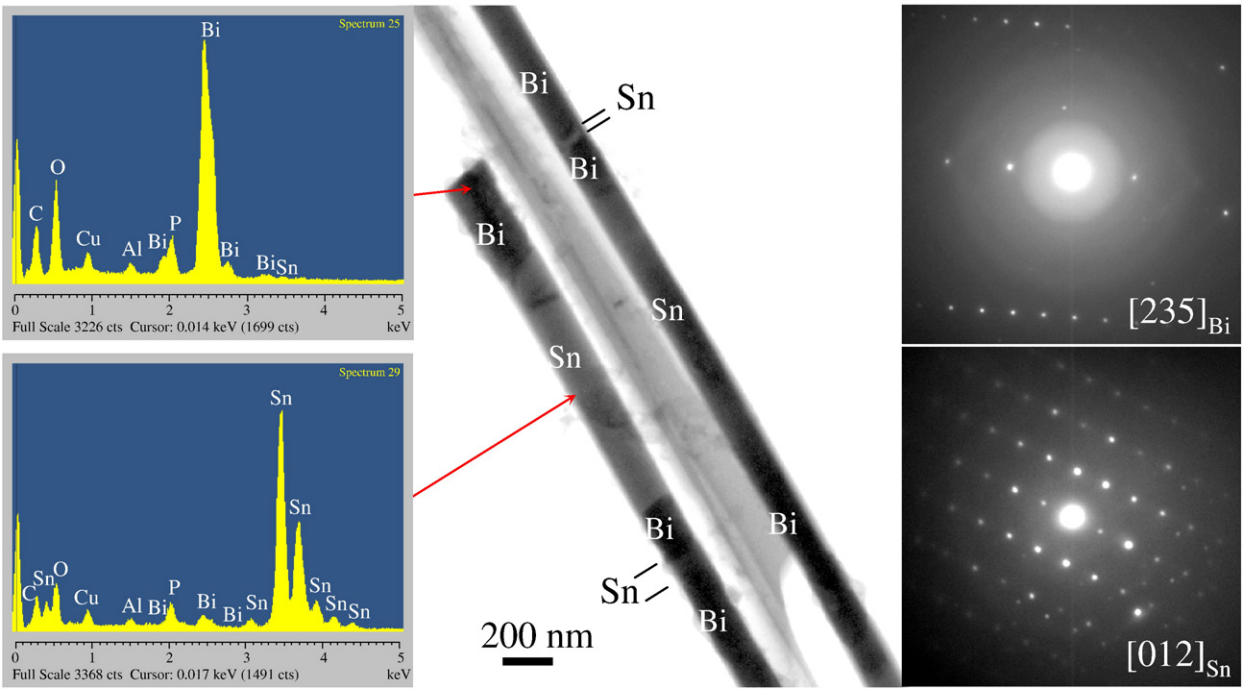

Fig. 3. TEM image and analyses of the 220 nm Bi–Sn eutectic nanowire.

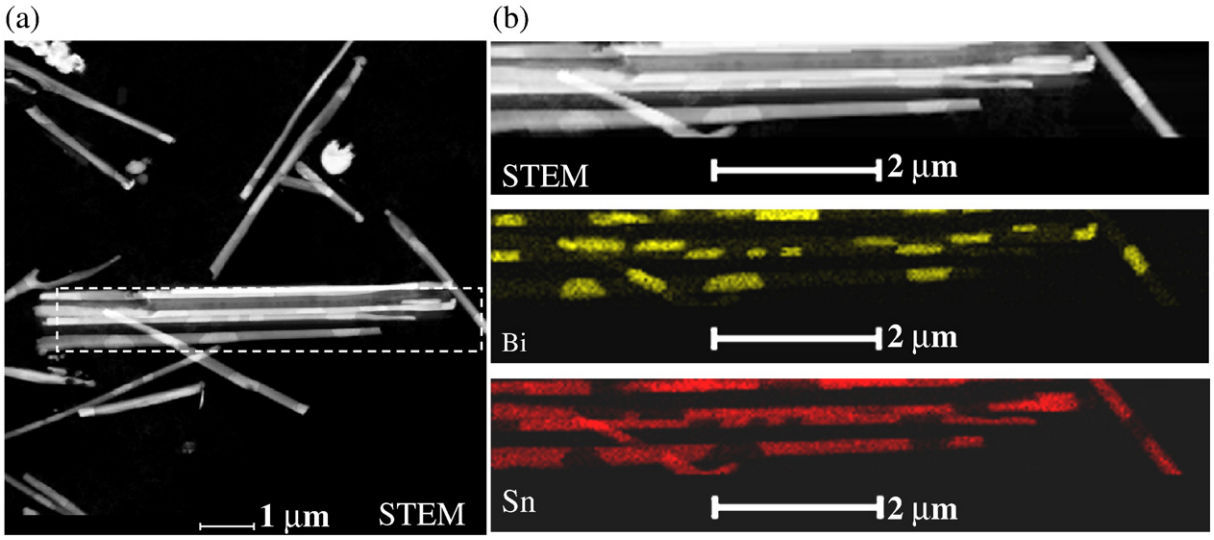

Fig. 4. (a) STEM image of the 220 nm Bi–Sn eutectic nanowire; (b) enlargement of the framed area in (a) along with the elemental maps Bi and Sn.

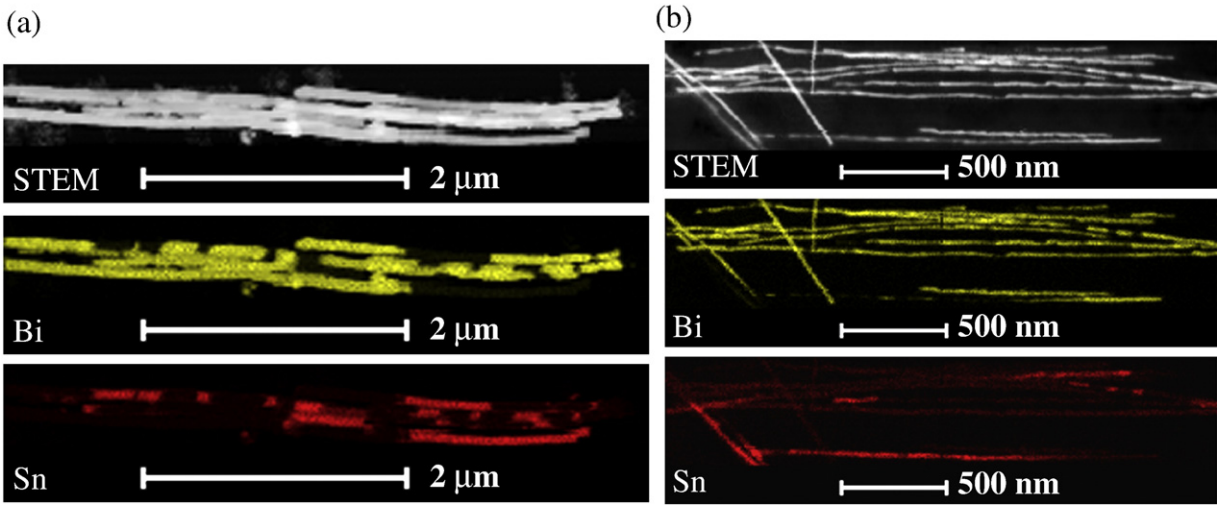

Fig. 5. STEM image and elemental maps of the 70 nm (a) and 20 nm (b) nanowire.

dependent, it can be applied to fabricate other nanowires with multiple components.

Acknowledgement

The FE-SEM acquisition at TAMU was supported by the NSF grand DBI-0116835, the VP for Research Office, and the Texas Eng. Exp. Station.

Appendix A. Supplementary data

Supplementary data associated with this article can be found, in the online version, at doi:10.1016/j.matlet.2009.02.019.

References

[1] Soloman HD. J Electron Packag 1989;111:75–82.
[2] Mei Z, Grivas D, Shine MC, Morris Jr JW. J Electron Mater 1990;19:1273–80.
[3] Kang SK, Sarkhel AK. J Electron Mater 1994;23:701–7.
[4] Frear DR, Jang JW, Lin JK, Zhang C. JOM 2001;53:28–32.
[5] Jeon YD, Nieland S, Ostmann A, Reichl H, Paik KW. J Electron Mater 2003;32:548–57.
[6] Goldstein JLF, Morris JW. J Electron Mater 1994;23:477–86.
[7] Chriaštel'ová J, Ožvold M. J Alloys Compd 2008;457:323–8.
[8] Ma GF, Zhang HL, Zhang HF, Li H, Hu ZQ. Mater Lett 2008;62:1853–5.
[9] Zhang ZB, Ying JY, Dresselhaus MS. J Mater Res 1998;13:1745–8.
[10] Sauer G, Brehm G, Schneider S, Nielsch K, Wehrspohn RB, Choi J, et al. J Appl Phys 2002;91:3243–7.
[11] Cronin SB, Lin YM, Rabin O, Black MR, Dresselhaus G, Dresselhaus MS, et al. Microsc Microanal 2002;8:58–63.
[12] Li L, Zhang Y, Li GH, Wang XW, Zhang LD. Mater Lett 2005;59:1223–6.
[13] Ye ZX, Zhang H, Liu HD, Wu WH, Luo ZP. Nanotechnology 2008;19:085709 (5 pages).
[14] Yang D, Meng GW, Han FM, Zhang LD. Mater Lett 2008;62:3213–6.
[15] Chen CC, Bisrat Y, Luo ZP, Schaak RE, Chao CG, Lagoudas DC. Nanotechnology, 2006;17:367–74.
[16] Bisrat Y, Luo ZP, Davis D, Lagoudas D. Nanotechnology 2007;18:395601 (6 pages).
[17] Chen CC, Chen JH, Chao CG. Jpn J Appl Phys 2005;44:1529–33.
[18] Williams DB, Carter CB. Transmission electron microscopy: a textbook for materials science. New York: Plenum Press; 1996. p. 581.